

## Supporting Information

### 9-Fluorenone and 9,10-Anthraquinone Potential Fused Aromatic Building Blocks to Synthesize Electron Acceptors for Organic Solar Cells

1. Figure S1.  $^1\text{H}$  NMR (400 MHz,  $\text{CDCl}_3$ ) spectrum of 5-(bromomethyl)undecane (**1**).
2. Figure S2.  $^1\text{H}$  NMR (400 MHz,  $\text{CDCl}_3$ ) spectrum of 2,5-bis(2-butyloctyl)-3,6-di(thiophen-2-yl)pyrrolo[3,4-*c*]pyrrole-1,4(2*H*,5*H*)-dione (**2**).
3. Figure S3.  $^1\text{H}$  NMR (400 MHz,  $\text{CDCl}_3$ ) spectrum of 3-(5-bromothiophen-2-yl)-2,5-bis(2-butyloctyl)-6-(thiophen-2-yl)pyrrolo[3,4-*c*]pyrrole-1,4(2*H*,5*H*)-dione (**3**).
4. Figure S4.  $^1\text{H}$  NMR (400 MHz,  $\text{CDCl}_3$ ) spectrum of 2,6-bis(4,4,5,5-tetramethyl-1,3,2-dioxaborolan-2-yl)anthracene-9,10-dione (**5**).
5. Figure S5.  $^1\text{H}$  NMR (400 MHz,  $\text{CDCl}_3$ ) and  $^{13}\text{C}$  NMR (100 MHz,  $\text{CDCl}_3$ ) spectra of 6,6'-(5,5'-(9-oxo-9*H*-fluorene-2,7-diyl)bis(thiophene-5,2-diyl))bis(2,5-bis(2-butyloctyl)-3-(thiophen-2-yl)pyrrolo[3,4-*c*]pyrrole-1,4(2*H*,5*H*)-dione) (**DPP-FN-DPP**).
6. Figure S6.  $^1\text{H}$  NMR (400 MHz,  $\text{CDCl}_3$ ) and  $^{13}\text{C}$  NMR (100 MHz,  $\text{CDCl}_3$ ) spectra of 6,6'-(5,5'-(9,10-dioxo-9,10-dihydroanthracene-2,6-diyl)bis(thiophene-5,2-diyl))bis(2,5-bis(2-butyloctyl)-3-(thiophen-2-yl)pyrrolo[3,4-*c*]pyrrole-1,4(2*H*,5*H*)-dione) (**DPP-ANQ-DPP**).
7. Figure S7. Photo-electron spectra (PESA) of (a) **DPP-FN-DPP** and (b) **DPP-ANQ-DPP**.
8. Figure S8. UV-Vis spectra of DPP-FN-DPP and DPP-ANQ-DPP thin films as-cast and after thermal annealing at 120 °C for 5 min.
9. Figure S9. Normalized EQE spectra.
10. Figure S10. UV-Vis spectra of as-cast and annealed blends.
11. Figure S11. GIWAXS scattering patterns of as-cast and annealed neat films.
12. Table S1. Properties of the out-of-plane P3HT (100) peak in as-cast and annealed films.
13. Fig. S12. Resonant soft X-ray scattering profiles of as-cast and annealed P3HT:**DPP-FN-DPP** and P3HT:**DPP-ANQ-DPP** blends.
14. Fig. S13. Computed UV-VIS spectra of **DPP-FN-DPP** and **DPP-ANQ-DPP** in chloroform.

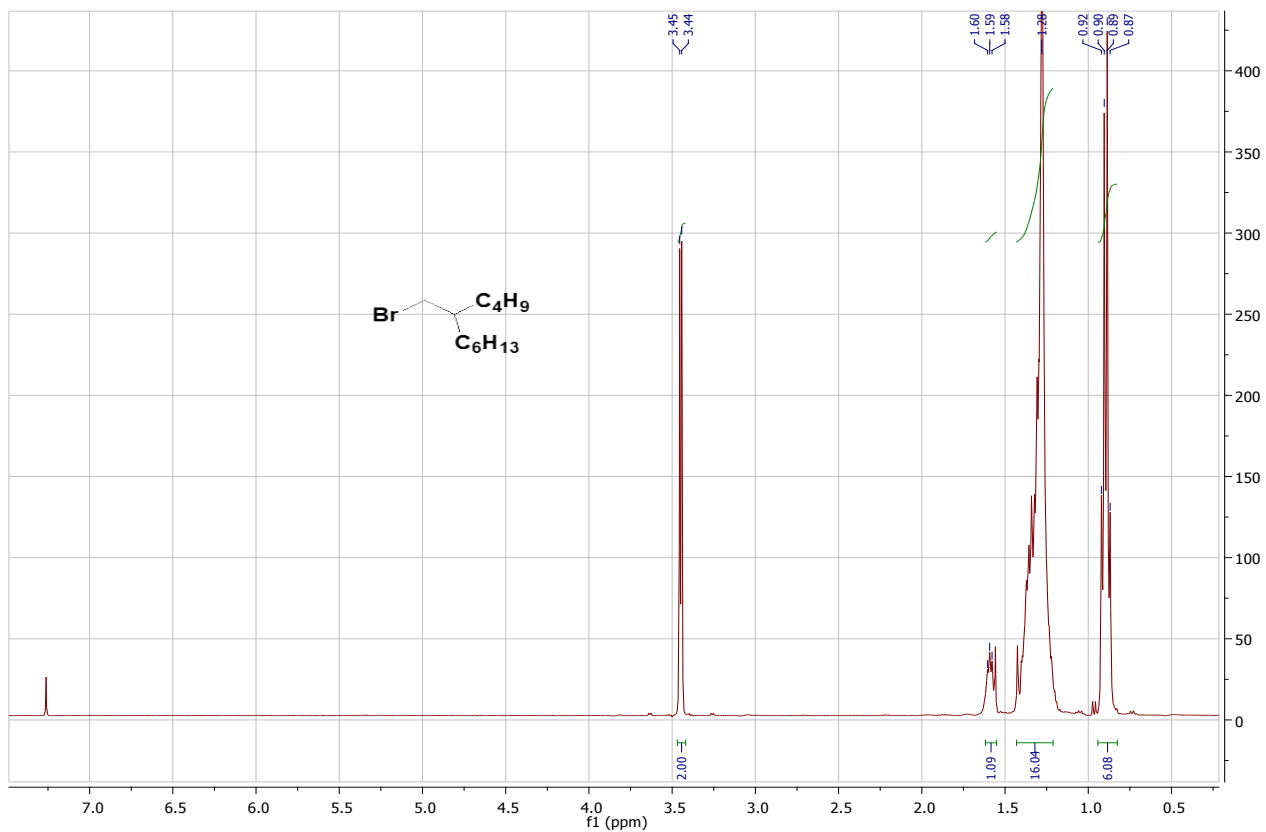


Figure S1.  $^1\text{H}$  NMR (400 MHz,  $\text{CDCl}_3$ ) spectrum of **1**

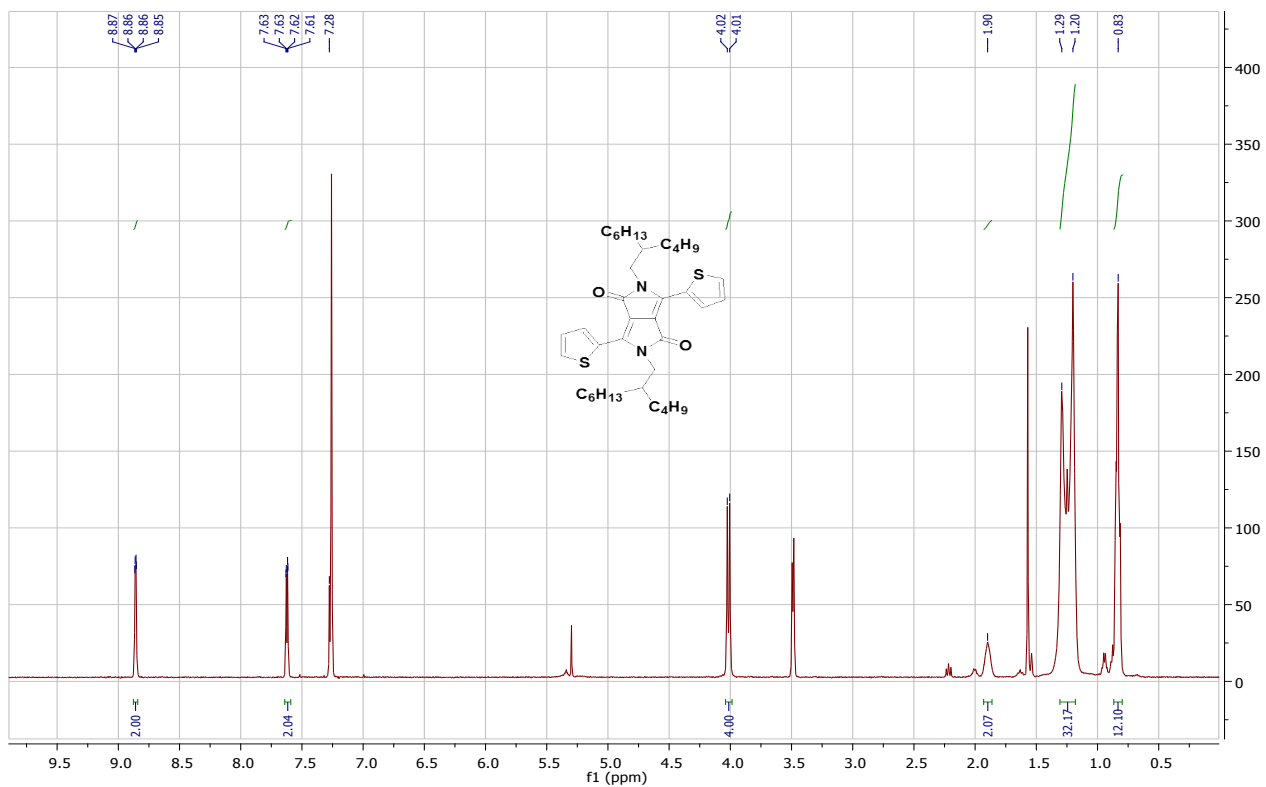
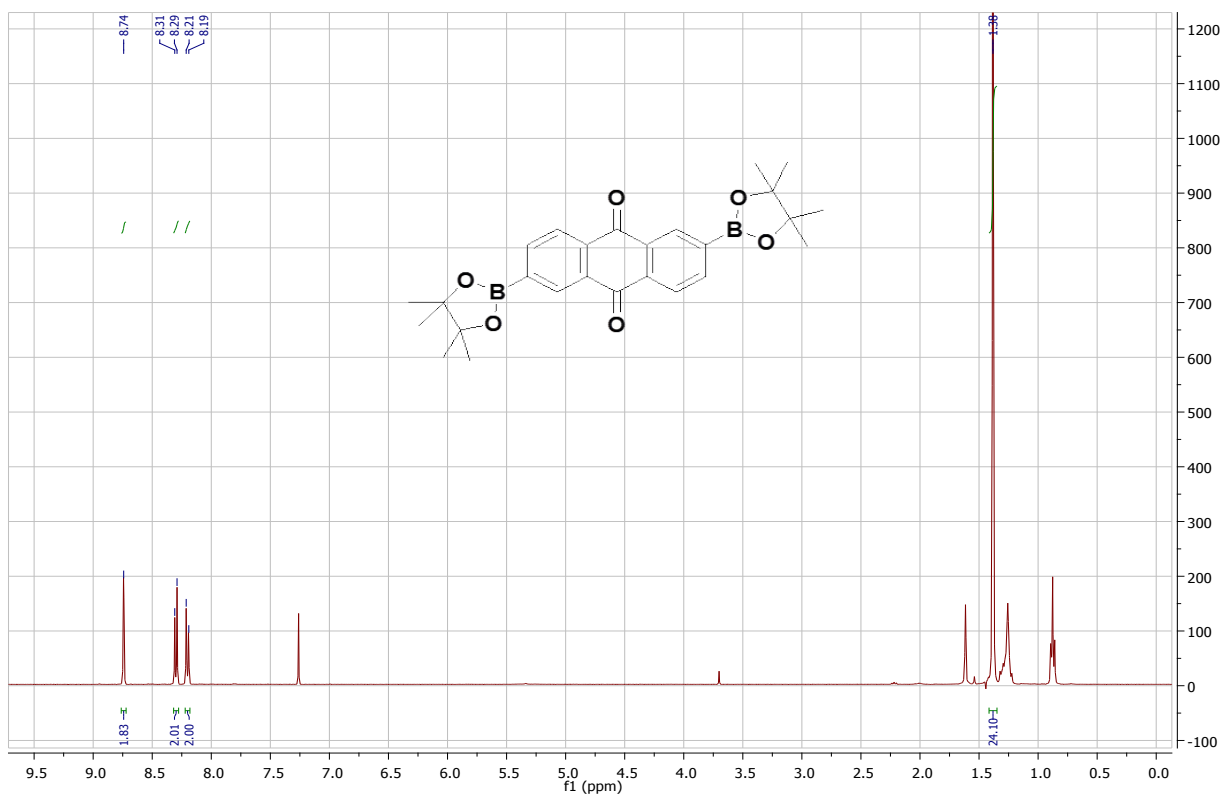
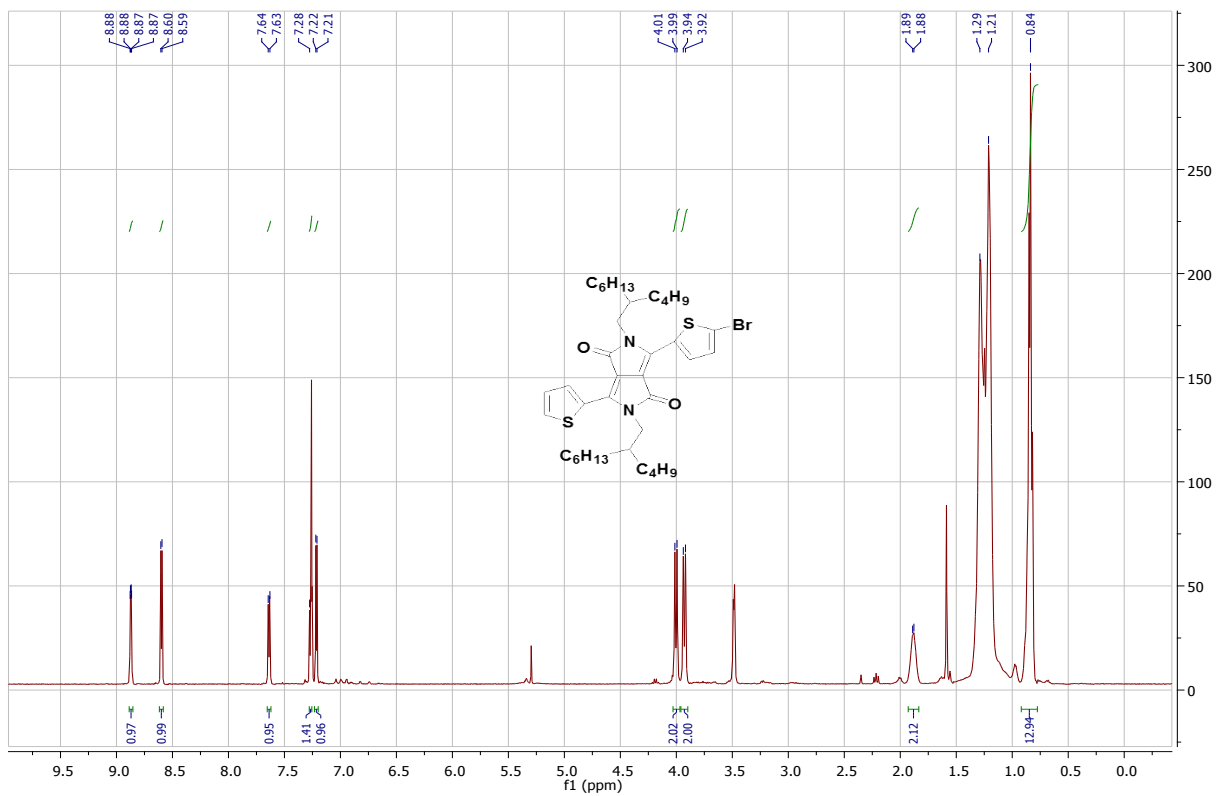


Figure S2.  $^1\text{H}$  NMR (400 MHz,  $\text{CDCl}_3$ ) spectrum of **2**



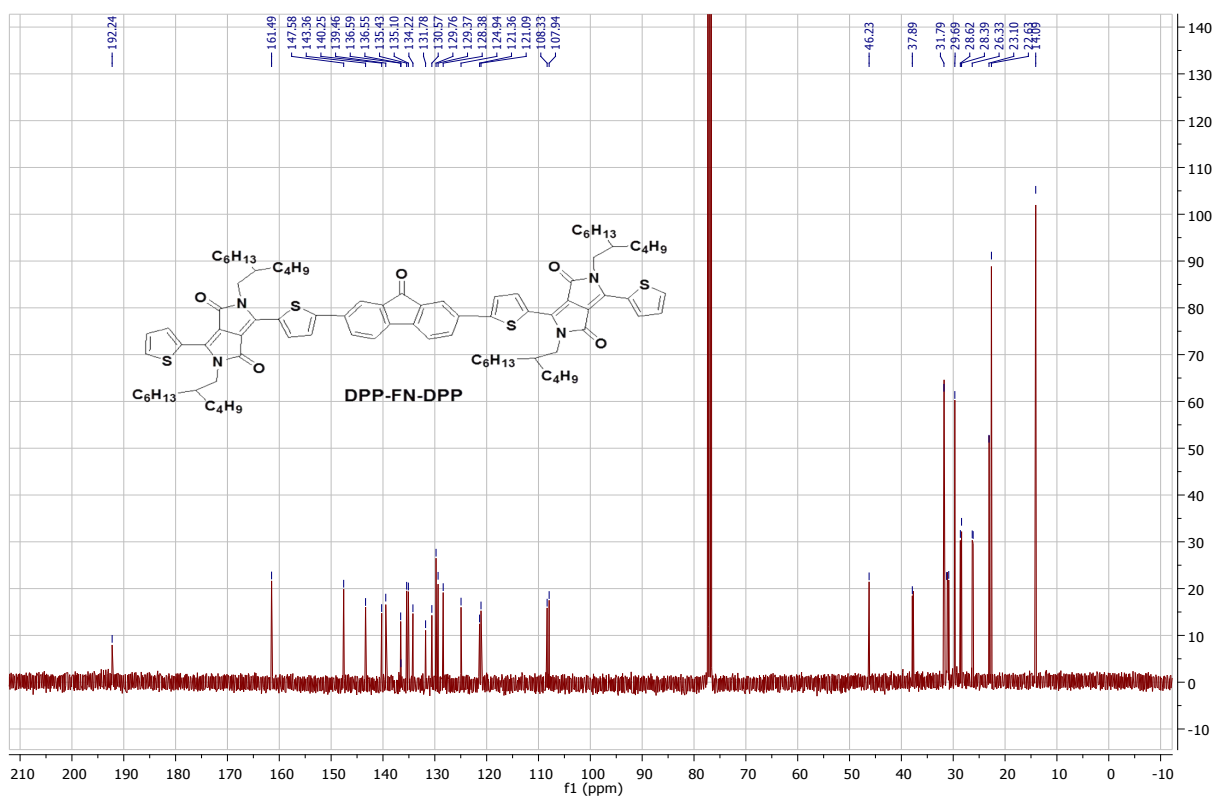
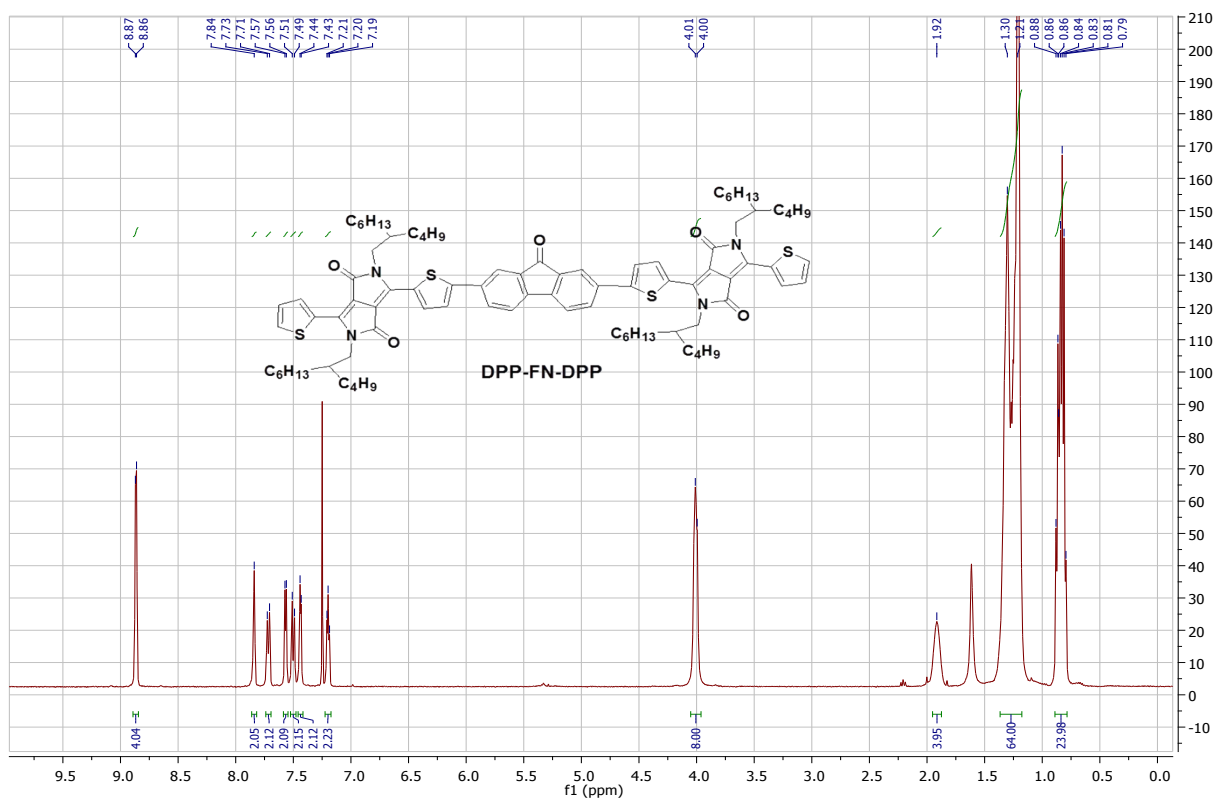


Figure S5. <sup>1</sup>H (400 MHz, CDCl<sub>3</sub>) and <sup>13</sup>C NMR (100 MHz, CDCl<sub>3</sub>) spectra of DPP-FN-DPP

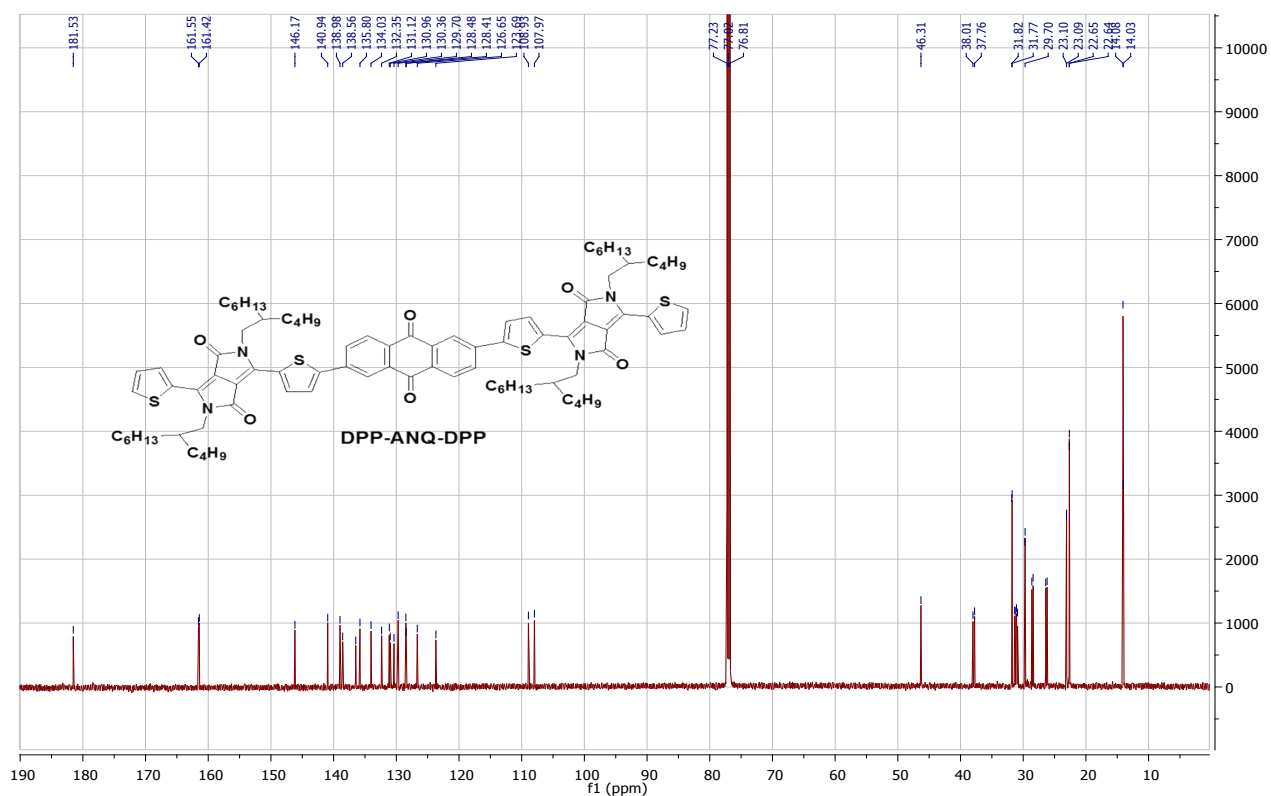
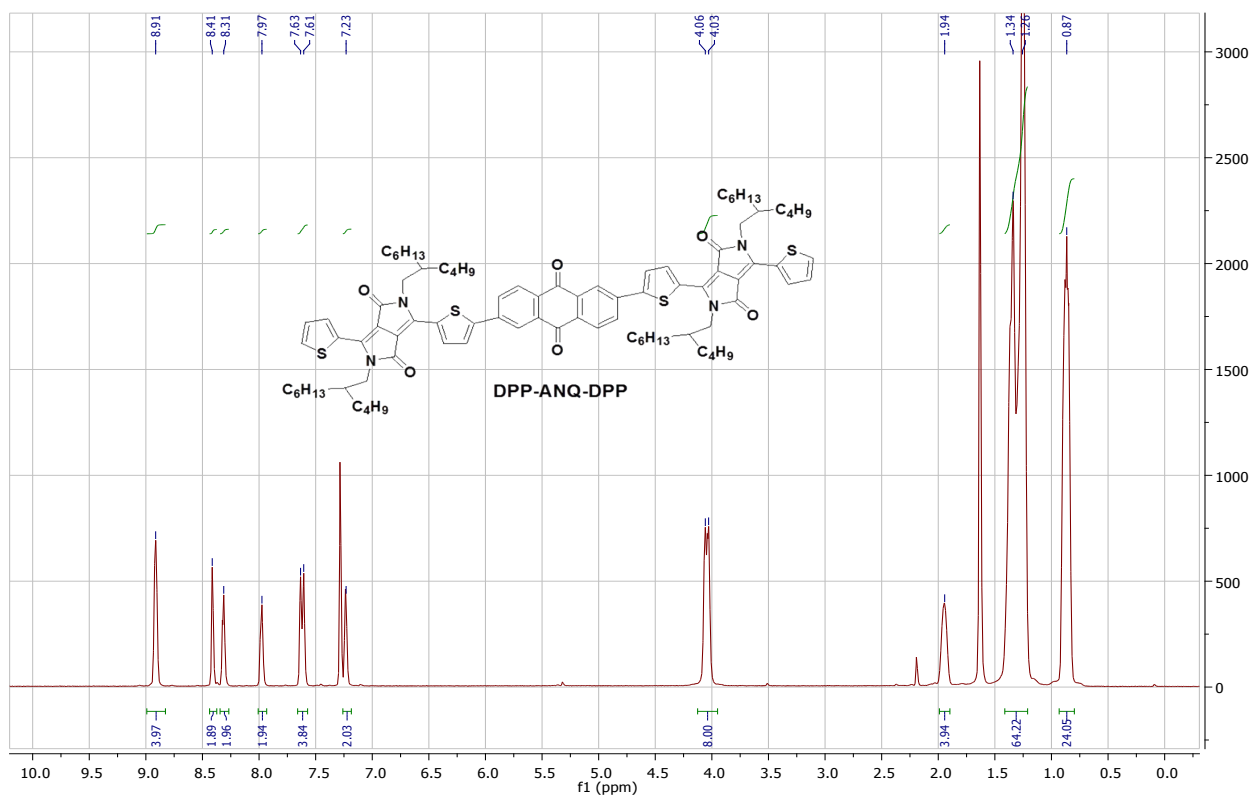


Figure S6. <sup>1</sup>H (400 MHz, CDCl<sub>3</sub>) and <sup>13</sup>C NMR (100 MHz, CDCl<sub>3</sub>) spectra of DPP-ANQ-DPP

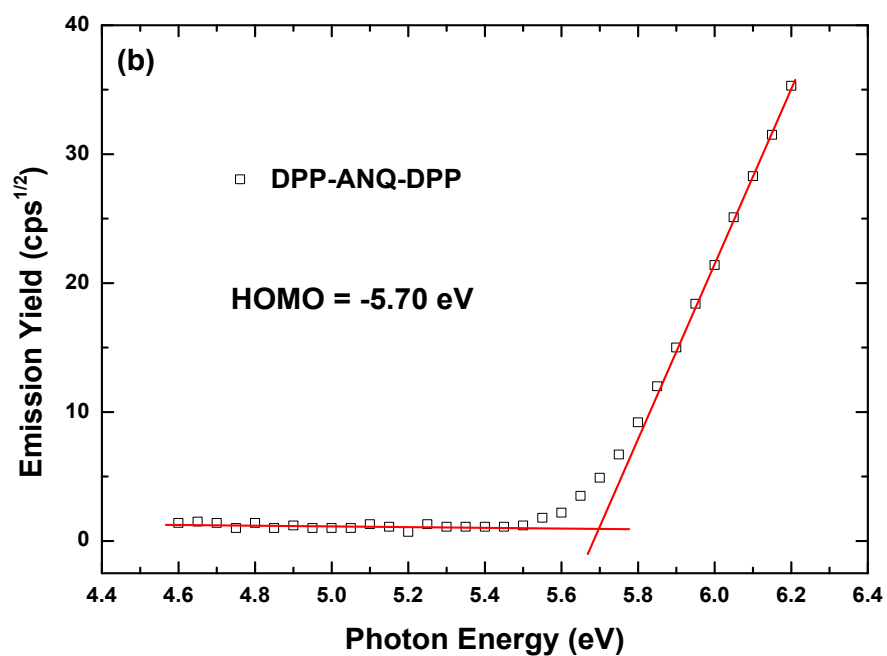
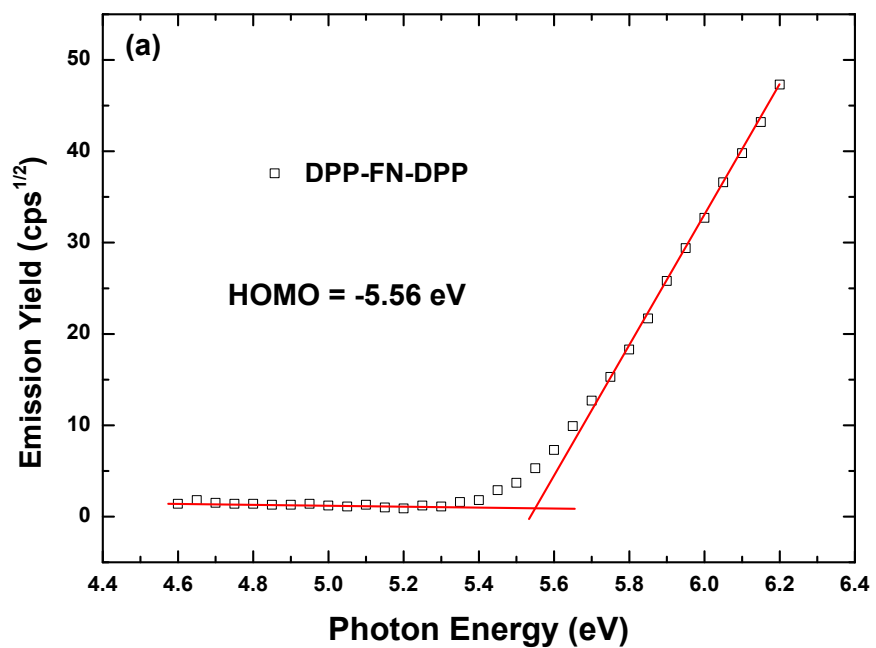


Figure S7. Photo-electron spectra (PESA) of (a) DPP-FN-DPP and (b) DPP-ANQ-DPP.

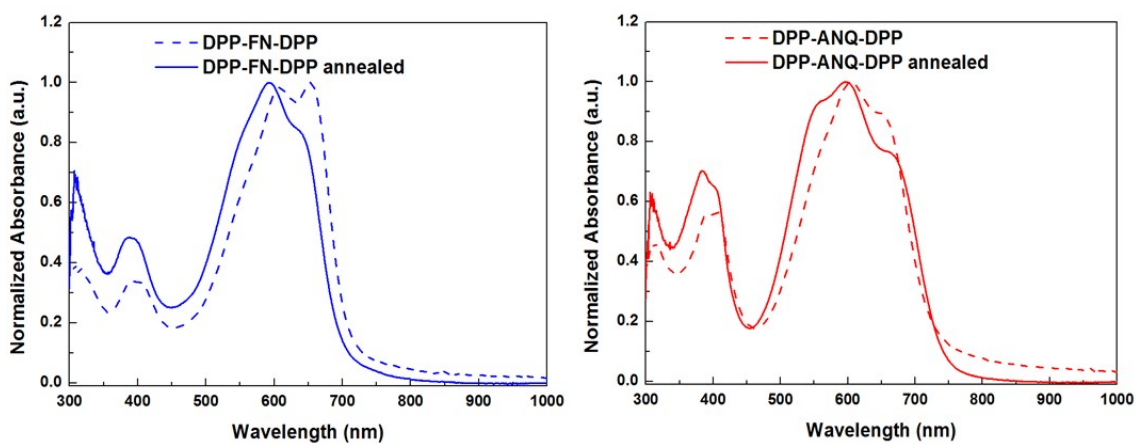


Figure S8. UV-Vis spectra of DPP-FN-DPP and DPP-ANQ-DPP thin films as-cast and after thermal annealing at 120 °C for 5 min.

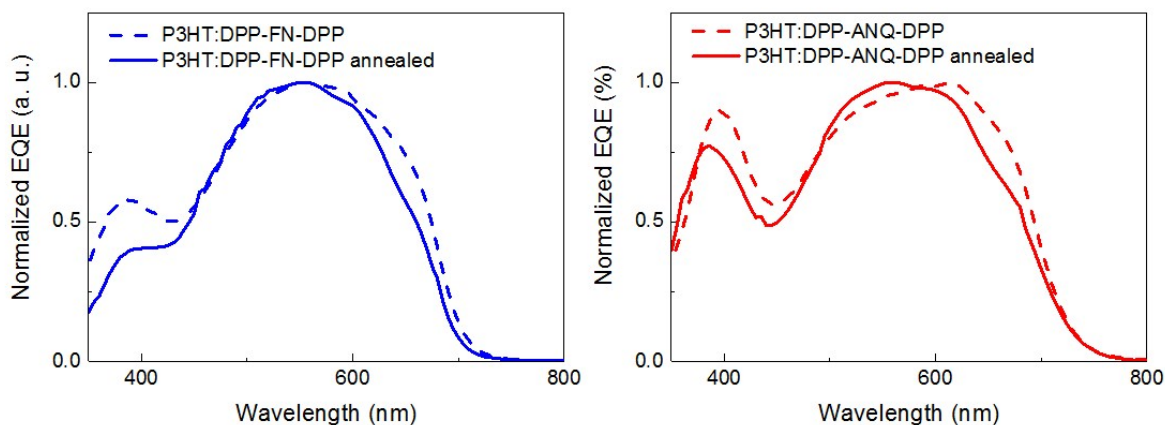


Figure S9. Normalized EQE spectra.

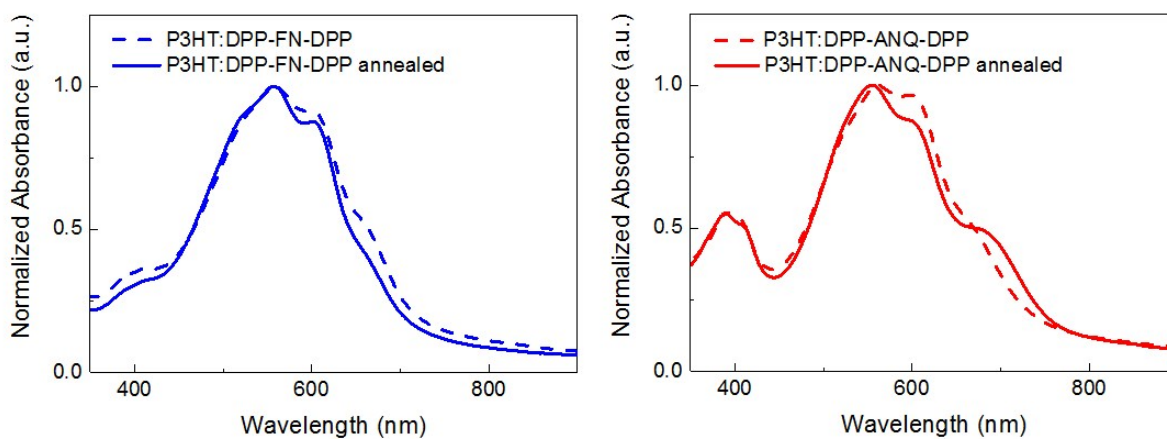


Figure S10. UV-Vis spectra of as-cast and annealed blends.

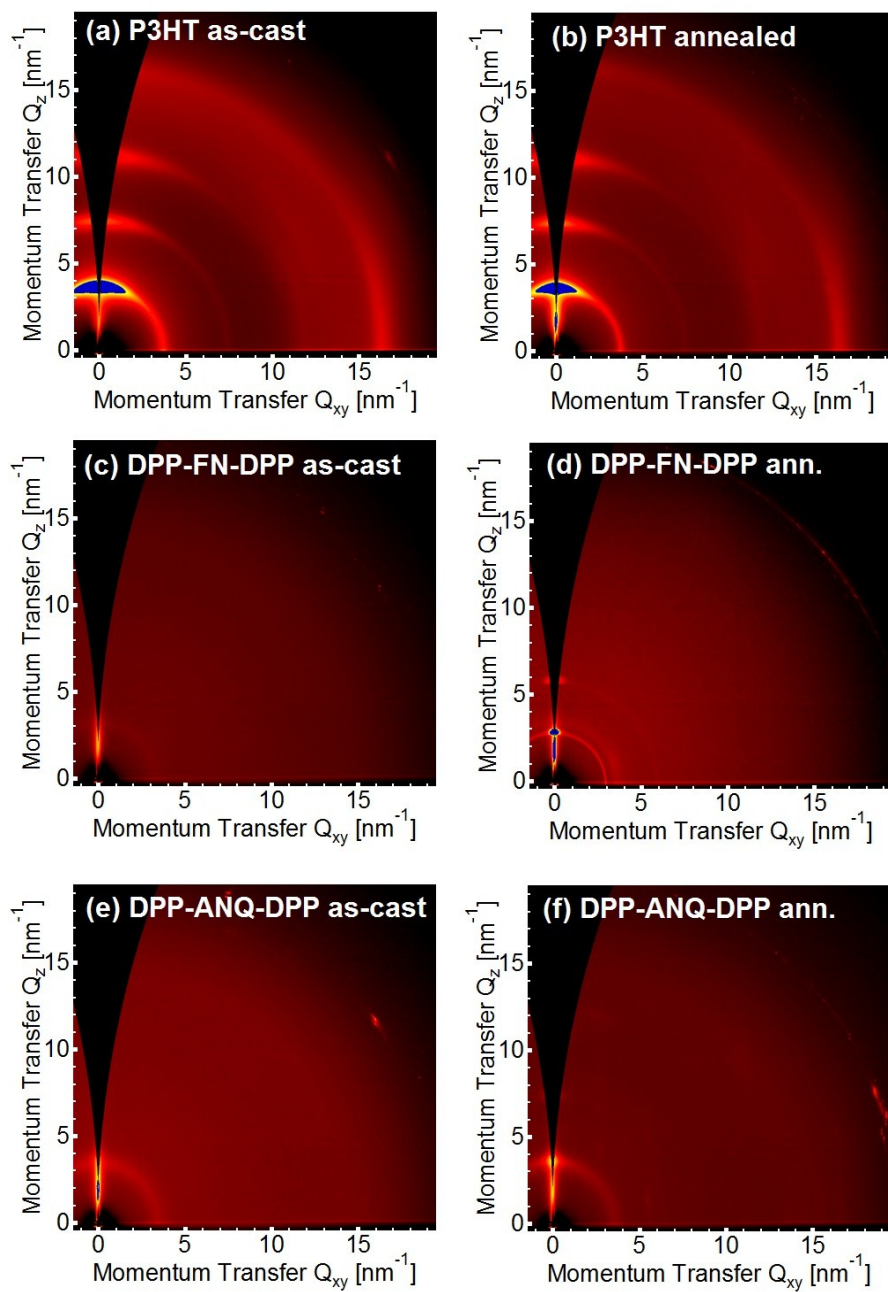


Figure S11. GIWAXS scattering patterns of as-cast and annealed neat films.

Table S1. Properties of the out-of-plane P3HT (100) peak in as-cast and annealed films.

	d-spacing (Å)	Coherence length (Å)	Area (a.u.)
P3HT:DPP-FN-DPP as-cast	$16.9 \pm 0.1$	$177 \pm 4$	$1370 \pm 30$
P3HT:DPP-FN-DPP ann.	$17.0 \pm 0.1$	$182 \pm 2$	$1400 \pm 15$
P3HT:DPP-ANQ-DPP as-cast	$17.1 \pm 0.1$	$94 \pm 1$	$156 \pm 2$
P3HT:DPP-ANQ-DPP ann.	$16.0 \pm 0.1$	$154 \pm 2$	$715 \pm 10$

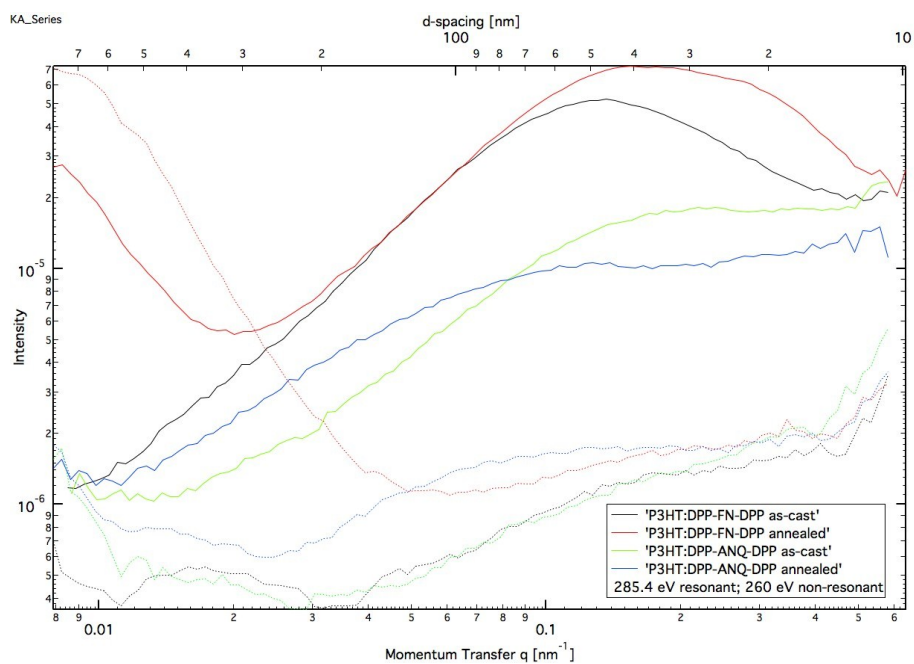
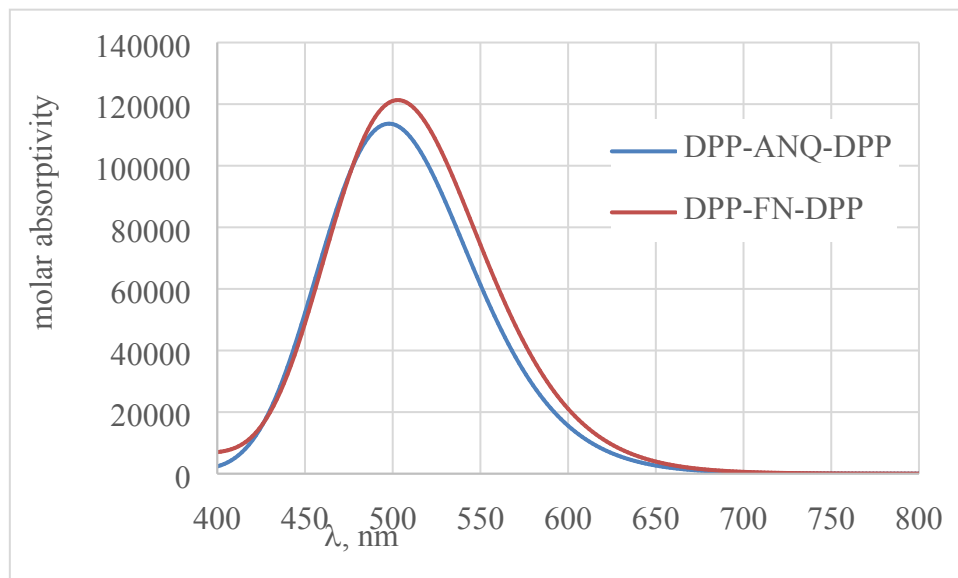


Fig. S12. Resonant soft X-ray scattering profiles of as-cast and annealed P3HT:DPP-FN-DPP and P3HT:DPP-ANQ-DPP blends. Resonant scattering traces (taken at 285.4 eV) are shown as solid lines while non-resonant scattering traces (taken at 260 eV) are shown as dashed lines.



*Fig. S13.* Computed UV-VIS spectra of **DPP-FN-DPP** and **DPP-ANQ-DPP** in chloroform. The excitations are predominantly HOMO-to-LUMO.